Laboratory Batch Reactor Method for Kinetic Study of Chemical Vapor Deposition

Carol M. McConica, David A. Bell, Kevin L. Baker, and Devin Moss
Dept. of Chemical and Bioresource Engineering, Colorado State University, Fort Collins, CO 80523

A lab-scale nonflowing reactor was built to study chemical vapor deposition reactions. Mass spectrometry is used to follow reaction pathways and to determine instantaneous reaction rates throughout film growth. In each experiment, the kinetic rate dependence on concentration for a wide range of concentrations is observed as reactants convert to products. This method of obtaining kinetic data is efficient in terms of sample loading, gas usage, and time, since over 200 instantaneous rate/composition pairs can be determined from one 30-min deposition. Because the rate is determined from gas–mass balance, rather than film-thickness measurements, an unlimited number of rate studies can be made on one sample. As a test case, the SiH_4 reduction of WF_6, used to deposit tungsten during integrated-circuit production, was investigated in the 0.64-L nonflowing laboratory reactor. Gas compositions were measured 2 mm from the growing surface, throughout time, with a mass spectrometer equipped with a capillary sampling tube. Tungsten was deposited on the 95°C surface, and $SiHF_3$ was the primary silicon fluoride reaction product for most tested conditions. A multiple-regression analysis of 1,975 instantaneous composition/rate pairs gives orders of 1.22 in silane, 0.27 in hydrogen, and −2.17 in WF_6. The ratio of SiF_4 to $SiHF_3$ stays low and constant until the gas becomes silane-rich. The evolution of the instantaneous rate over time implies that a minimal level of thermal activation of the reactive gases is necessary for the deposition to be surface-rate-limited. Preliminary heat-transfer models of the wire substrate imply that heat transfer to the gas phase is in the Knudsen regime.

Introduction

Chemical vapor deposition (CVD) is a commonly used technique for depositing thin films during the manufacturing of integrated circuits (IC). The optimization of the deposition process is enhanced by a knowledge of the reaction kinetics. It has been the tradition in the IC industry to attempt to determine reaction kinetics from film thickness measurements taken at the end of a deposition in a flowing reactor that operates at steady state. The near-wafer gas composition is rarely measured. Most authors correlate inlet flow rates and total pressure to film thickness, without any knowledge of the true chemical composition driving film growth. An optimal set of flow rates in one reactor does not transfer to another reactor because the hardware results in different reactant conversions and transport phenomena effects. Kinetic studies are best performed in a reactor where the instantaneous rate is determined from the dynamics of the chemical species and correlated with the actual chemical environment, as measured near the growing film. The instantaneous film growth rate can be determined from a mass balance on the instantaneous near-surface gas composition. The integrated film depth can be confirmed with postdeposition thickness measurements.

A CVD reactor has been designed and built where the near-surface chemical environment of the process is observed and can be used to determine reaction pathways and chemical kinetics. The test vehicle for the reactor was the deposition of tungsten by the silane reduction of tungsten hexafluoride. Tungsten is typically deposited by the reduction of gaseous tungsten hexafluoride (WF_6) with hydrogen (H_2) or silane (SiH_4). Published studies of SiH_4/WF_6 reaction kinetics present conflicting results. A review and analysis by Shon (1992) showed that most of the published data were taken under mass transfer limited conditions. Consequently, these

Current address of D. A. Bell: Dept. of Chemical and Petroleum Engineering, University of Wyoming, P.O. Box 3295, Laramie, WY 82071.

are not valid kinetic studies. A notable exception is the recent paper by Ammerlaan et al. (1993). They measured rates of weight gain for samples suspended from a microscale balance. For SiH_4/WF_6 pressure ratios less than 0.3, they found a 1.06 reaction order for SiH_4 and a -0.16 reaction order for WF_6. For SiH_4/WF_6 pressure ratios between 0.3 and 1.0, they found a 1.82 reaction order for SiH_4 and a -0.94 reaction order for WF_6.

The reaction pathway has also remained undefined, since most deposition studies do not include observation of chemical products. Silicon tetrafluoride (SiF_4) was long presumed to be a major reaction product of the SiH_4/WF_6 reaction:

$$2WF_6(g)+3SiH_4(g)\rightarrow 2W(s)+3SiF_4(g)+6H_2(g). \quad (1)$$

Other proposed reactions list hydrogen fluoride (HF) as a reaction product. Kobayashi et al. (1991) used infrared spectroscopy to show that under conditions of high partial pressures of WF_6, silicon hydrogen trifluoride ($SiHF_3$) is a major product and that SiF_4 is a minor product:

$$WF_6(g)+2SiH_4(g)\rightarrow W(s)+2SiHF_3(g)+3H_2(g). \quad (2)$$

Kobayashi et al. (1991) noted that mass spectroscopy is the most common technique used to monitor CVD reactor gas phase compositions and that the SiF_3^+ ion, which most investigators presumed to be a cracking fragment of SiF_4, is also a cracking fragment of $SiHF_3$.

Cheek et al. (1993) have shown that either $SiHF_3$ or SiF_4 can be a major reaction product, depending upon the reaction conditions. They used a mass spectrometer equipped with a capillary sampling tube to measure near-surface concentrations of $SiHF_3$ and SiF_3 during deposition. The mass 67 ($SiHF_2^+$) to mass 85 (SiF_3^+) signal ratio declined with increasing SiH_4/WF_6 feed ratios up to a 1.3 feed ratio, and then increased. Schmitz et al. (1989) showed that selective deposition (a catalytically induced deposition on silicon or metals, but not silicon dioxide) occurs over a limited range of SiH_4/WF_6 feed ratios, and at high SiH_4/WF_6 feed ratios, tungsten silicide rather than tungsten deposits. Cheek et al., noted that changes in the $SiHF_2^+/SiF_3^+$ ratio correspond to changes in deposition behavior, and suggest the use of near-surface mass-spectrometer measurements as a means of real-time process control.

In this study, a batch laboratory reactor was used to observe SiH_4/WF_6 reactions. Unlike most CVD reactors, in which reactant gases continually flow through the reactor, gases were added to the ambient temperature reactor in batch mode. This allows observation of hundreds of composition-rate pairs as the reactants convert to products. A mass spectrometer equipped with a capillary sampling tube, similar to the device used by Cheek et al., is used to measure near-surface gas partial pressures of several species throughout time.

Experimental Methods

Apparatus

The experimental apparatus is shown in Figure 1. The heated reaction surface consists of a resistively heated tungsten wire, 0.76 mm diameter by 10.6 cm long. The volume of the reactor is 0.64 L. Due to the pyrophorric nature of SiH_4, this gas is fed to the reactor as a 5% SiH_4/95% He mixture. Nominal reaction temperatures are measured with a Type K thermocouple spot-welded to the tungsten wire, 4.1 cm from one end. The base pressure of the reactor is 10^{-7} torr.

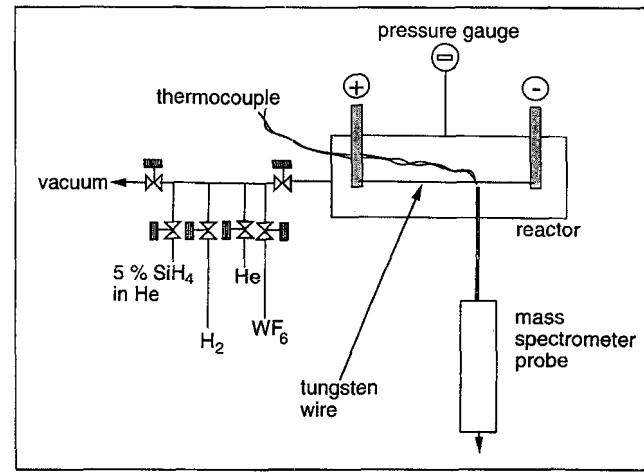

Figure 1. Laboratory batch reactor.

Gas compositions are measured with a quadrupole mass spectrometer (Balzers QMG 420) with a 0–200 amu range and a fixed, 100-V electron-impact ionization energy. The mass spectrometer is controlled via a software program on an IBM-compatible personal computer that allows the spectrometer to rapidly cycle between discreet mass values and record the measured signals to a disk drive. The reactor and the mass spectrometer are evacuated by separate turbomolecular vacuum pumps, each backed by an oil-sealed rotary-vane vacuum pump.

The mass spectrometer is equipped with a 1.59-mm OD by 0.51-mm ID by 15-cm-long nickel capillary sampling tube (Aesar). The tube inlet is positioned 1 to 2 mm away from the wire surface at the point where the thermocouple is spot-welded to the tungsten wire. Flow through the tube is adjusted prior to the experiments by crimping the tube inlet. Since the primary restriction to flow through the capillary is the crimped inlet, rather than the body of the capillary, the gas pressure within the capillary is closer to the mass-spectrometer pressure (10^{-5} torr or less) than the reactor pressure (2 torr or higher). The small quantity of gas within the sampling tube is pumped through the mass spectrometer by a 50-L/s turbomolecular vacuum pump, so the mass spectrometer rapidly responds to changes within the reactor.

Temperature and mixing transients

The reactor is charged by first adding WF_6, then H_2, and finally the 5% SiH_4 mixture. After all of the reactants are charged to the reactor, and allowed to intermix, the wire temperature is raised to a nominal 95°C.

Preliminary mixing experiments were run to measure the time required for the gases to intermix and approach thermal equilibrium. Figure 2 shows an experiment in which 6 torr H_2 was charged to the reactor, followed by 2 torr WF_6. Since the capillary inlet is near the end of the reactor furthest from the inlet valve, the H_2^+ signal rises as the WF_6 compresses the

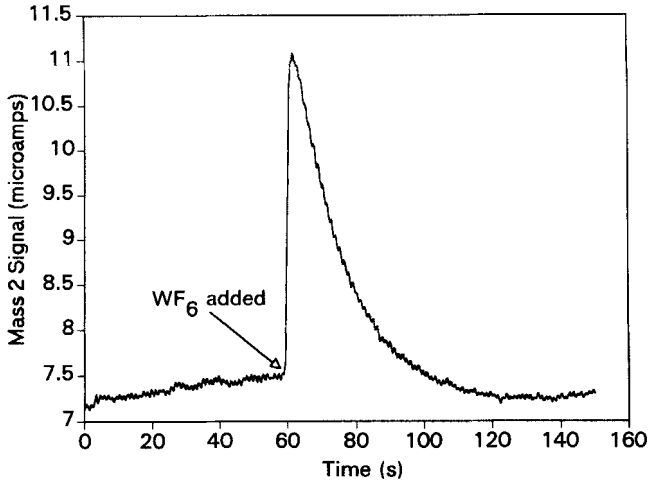

Figure 2. Change in mass 2 (H_2^+) signal when 2 torr of WF_6 was added to 6 torr of H_2 in the reactor.

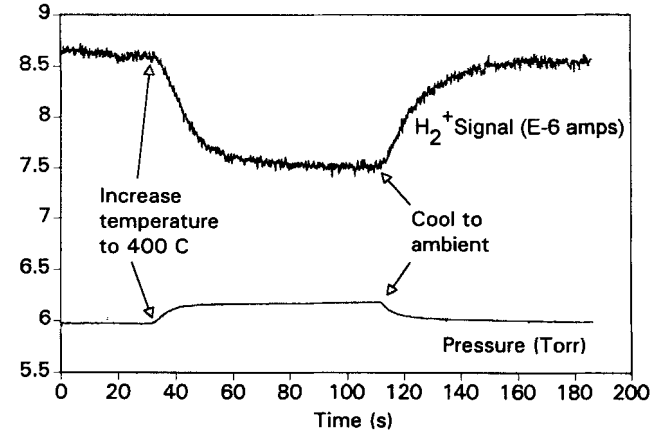

Figure 3. Change in H_2^+ mass spectrometer signal and reactor pressure when tungsten wire was heated from ambient temperature to 400°C and then allowed to cool to ambient.

H_2 near the sampling point. As the WF_6 and H_2 interdiffuse, the H_2^+ signal falls to its former level. After about 50 s, the two components were well mixed. Because the deposition reactions were run at lower total pressures, this time for intermixing represents an upper limit.

Figure 3 shows an experiment in which 6 torr of H_2 was charged to the reactor at ambient temperature. The wire temperature was then raised to a nominal 400°C, and held at that temperature for about 55 s. The wire was then allowed to cool to ambient temperature. When the wire was heated, the reactor pressure rose and the H_2^+ signal fell, both due to thermal gas expansion. New steady-state pressure levels were attained after about 50 s. Experiments were run over a range of gas pressures and wire temperatures. Data from these experiments were used to develop an empirical correlation for gas expansion that was then used to correct mass-spectrometer signal to partial-pressure conversion factors.

Wire temperature profile

Work is currently underway to model the temperature profile of the wire substrate. Moss (1995) developed, solved, and compared a simplified model for the wire-temperature profile with experimental measurements for the case of an evacuated reactor.

For any small axial element of the wire, a heat balance must consider heat conduction through the wire to the electrodes, radiation directly to the inside wall of the reactor, and heat generation by electrical power dissipation. Because the wire reaches its steady-state temperature within 10 s, accumulation of heat is ignored in the model. A heat balance, given in Carslaw and Jaeger (1959), which invokes Fourier's law and neglects radiation effects at 95°C, results in:

$$\frac{d^2T}{d\gamma^2} + \frac{I^2\rho L^2}{kA^2} = 0, \tag{3}$$

where T is the wire temperature, γ is dimensionless wire length, I is the current supplied to the wire, ρ is the measured resistivity of 8.43×10^{-8} Ω-m, L is the half-length of the wire or 0.052 m, k is the thermal conductivity of tungsten or 170.3 $W \cdot m^{-1} \cdot K^{-1}$, and A is the wire cross-sectional area given as 4.56×10^{-7} m^2.

The boundary conditions are that the ends of the wire be at the measured electrode temperature and a maximum temperature exist at the wire center:

$$T = T_{\text{electrode}} \qquad \text{at } \gamma = 0$$

$$\frac{dT}{d\gamma} = 0 \qquad \text{at } \gamma = 1.$$

In vacuum, this simple model has an analytical solution that predicts the wire temperature as a function of dimensionless distance from the electrode:

$$T = \frac{I^2\rho L^2}{2kA^2}(2\gamma - \gamma^2) + T_{\text{electrode}}.$$

When gases are added to the reactor, a heat balance that includes conduction to the gas, Q_{gas}, must be solved numerically:

$$\frac{d}{d\gamma}\left(kA\frac{dT}{d\gamma}\right) + \frac{I^2\rho L^2}{A} - \frac{PL^2Q_{\text{gas}}}{A} = 0. \tag{4}$$

The boundary conditions are the same as those given earlier. In this case, Q_{gas} was adjusted until the model predicted the measured wire center temperature. Experiments and calculations were run for a range of gas pressures and wire temperatures. To ease comparison between experiment and theory, only hydrogen was added to the reactor.

Experimental matrix and run procedure

A statistically designed set of experiments was run in which the independent variables were the initial SiH_4, WF_6, and H_2 partial pressures. Two levels of each variable, as shown in Table 1, were run, and all but one of the eight possible variable combinations were run twice. In addition, the center-

Table 1. Prereaction Partial Pressures of Reactants in Torr

	SiH_4*	WF_6	H_2	Total Pres.
High level	0.2	0.2	1.0	5.4
Low level	0.1	0.1	0.25	2.45
Center point	0.15	0.15	0.5	3.35

*Injected as 5% SiH_4/95% He mixture. Total pressure of this mixture was 20 times the SiH_4 partial pressure shown in the table.

point condition was run four times, for a total of 19 runs. The run order was randomized to prevent misinterpretation of time-dependent change.

To ensure a consistent initial surface for each experiment, a surface preparation run was completed prior to every experimental run. For each of these preparation runs, 0.4 torr of WF_6 was added to the reactor, followed by 0.4 torr of SiH_4. The reactants were allowed to interdiffuse for 240 s, and then the nominal wire temperature was increased to 250°C and held at that temperature for 390 s. The reaction was essentially complete within the first 100 s. The reactor was then evacuated to a base pressure of 5×10^{-7} torr before beginning each experimental run.

For each experimental run, the reactor was first charged with the desired WF_6 pressure and then with H_2. The data logging program was started, and after logging data for 20 s the reactor was charged with SiH_4. The reactants were allowed to intermix for 240 s before the wire temperature was raised to a nominal 95°C and held at that temperature for 1,060 s. Data logging was then stopped, the wire was allowed to cool, and then the H_2 calibration procedure described in the next section was carried out. Data taken for 130 s after the wire temperature was raised were not used in subsequent analyses to avoid complications due to thermal transient effects.

In preliminary experiments at center-point initial pressures, a range of wire temperatures was tested. The nominal 95°C reaction temperature was chosen because, after 200–400 data points, over half of the reactants were consumed, but there were sufficient remaining reactants to ensure that the reaction was not yet limited by diffusion of low concentration species to the surface.

Data analysis

Partial-Pressure Estimation. Table 2 shows the ions tracked during the experiments and their parent molecules. The WF_3^{++}, WF_4^{++}, and W^+ ions, cracking fragments of WF_6, could also be detected, but signal/noise ratios were poor, so quantitative measurements for WF_6 were not possible with this spectrometer. More abundant fragments of WF_6, such as the WF_5^+ ion, were outside the range of the 200-amu spectrometer. Partial pressures for WF_6 were estimated from initial WF_6 partial pressures, estimated silicon fluoride partial pressures, and the stoichiometry in Eqs. 1 and 2.

Table 2. Ions Tracked by Mass Spectrometer

Mass/Charge	Ion	Parent Molecule
2	H_2^+	H_2
31	SiH_3^+	SiH_4
67	$SiHF_2^+$	$SiHF_3$
85	SiF_3^+	$SiHF_3$,SiF_4

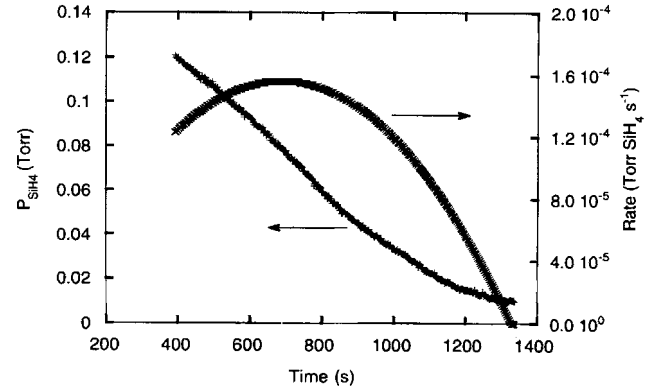

Figure 4. Silane partial pressure vs. time and calculated instantaneous rates for one characteristic experiment.

At the end of each experiment, the reactor was evacuated and the H_2^+ signal height was measured. The reactor was filled with 1 torr H_2, and the H_2^+ signal height was again measured. These two H_2^+ measurements provided H_2^+ signal to H_2 partial-pressure conversion factors and a measure of mass-spectrometer multiplier performance for each run. The SiH_4 partial pressure was also adjusted for multiplier performance, thermal effects, and conversion due to reaction.

Instantaneous Reaction Rate Analysis. To estimate instantaneous reaction rates for the 95°C reaction, plots of SiH_4 partial-pressure vs. time were constructed. A polynomial expression with the following form was then correlated to the data, where f, g, and h are fitting constants:

$$SiH_4 \text{ partial pressure} = f + g(\text{time}) + h(\text{time})^2 + \cdots. \quad (5)$$

Third- or fourth-order polynomials with r^2 values in excess of 0.99 were used. The instantaneous reaction rate was defined as the instantaneous rate of SiH_4 consumption and calculated by taking the derivative of Eq. 5:

$$r = -d(SiH_4 \text{ partial pressure})/dt = -g - 2(h)(\text{time}). \quad (6)$$

Since SiH_4 appears to be consumed by a single reaction, shown in Eq. 2, for most of the experiments at 95°C, this definition of reaction rate is proportional to the rate of tungsten deposition. An example of this analysis is shown in Figure 4, which plots silane partial-pressure measurements and the calculated instantaneous rate vs. time. The integrated-film growth rate can be determined by measuring the wire diameter change and dividing by the time of deposition, as shown in Figure 5. The rate profiles in this example are not axially symmetric due to gas convection resulting from the vertically oriented reactor operating at high pressure.

Results

Temperature profile model

The simplified wire heat balance for vacuum conditions

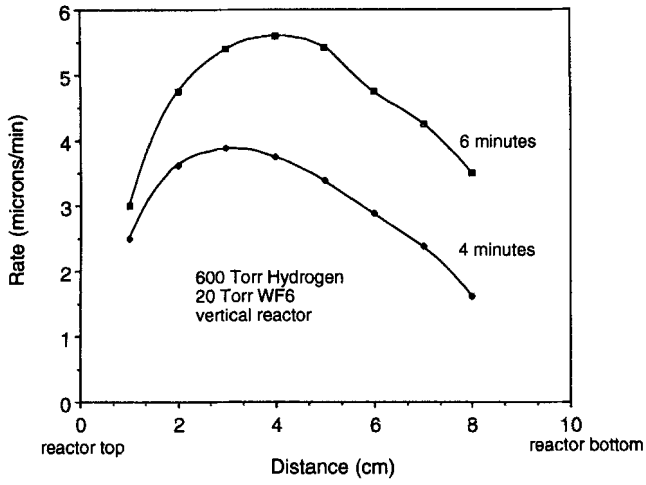

Figure 5. Wire growth as a function of axial position.

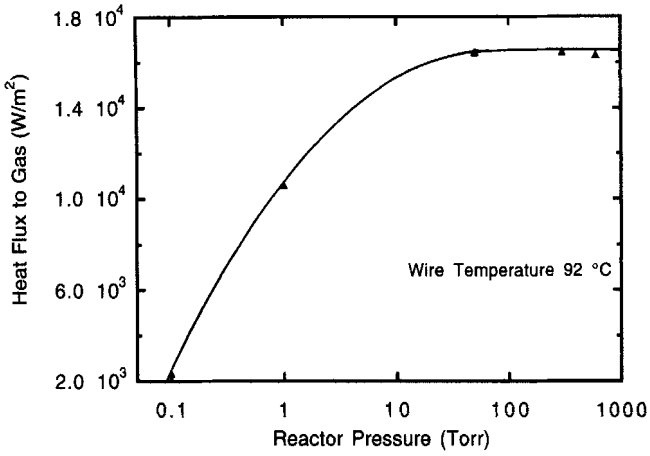

Figure 7. Heat flux from the wire center to the hydrogen gas as a function of pressure for a 92°C wire.

(Eq. 3) was used to predict the wire center temperature for a range of electrical currents. The calculated wire profile and measured center temperature in Figure 6 for a current of 4.35 amp result in a measured temperature of 95°C. There is excellent correspondence between model and experiment, validating the heat balance in vacuum.

Results from the more complex model, including conduction to the gas, are shown in Figure 7. The figure plots the calculated heat flux to the gas over a range of hydrogen pressures. It can be seen that the heat flux drops dramatically below 20 torr for a 92°C wire. Above 20 torr, the flux (loss to the hydrogen gas) is independent of pressure. Figure 8 plots the heat flux to the gas as a function of wire temperature for 1 and 50 torr. In continuum theory, heat flux should be independent of pressure and proportional to the temperature gradient ($T_{wire} - T_{wall}$). Both figures show that at low pressure, the heat flux depends on pressure when given one value for the wire–wall gradient. It is apparent that heat flux from the wire to the gas is in the Knudsen regime under the conditions of these kinetic experiments in this batch reactor.

Reactions at 95°C

The $SiHF_2^+/SiF_3^+$ ion ratio resulting from the 95°C reaction is nearly constant for 17 of the 19 experiments. The average $SiHF_2^+/SiF_3^+$ ratio is 1.29, and the standard deviation is 0.08 for the 17 experiments that exhibit this straight-line behavior. This constant ratio over a range of conditions suggests that this ratio is the mass-spectrometer cracking pattern for $SiHF_3$, and that this species is the only silicon fluoride reaction product. X-Ray microanalysis of the wire showed that tungsten was deposited.The two experiments that did not yield a constant $SiHF_2^+/SiF_3^+$ ratio were run under conditions of WF_6 surface starvation, where tungsten silicide rather than tungsten has been shown to be deposited (Schmitz et al., 1989).

Reaction orders

Reactors that are run in batch mode (no inlet or outlet flows) are ideal for determining reaction kinetics (Fogler, 1992). The gas composition can be measured over time, and

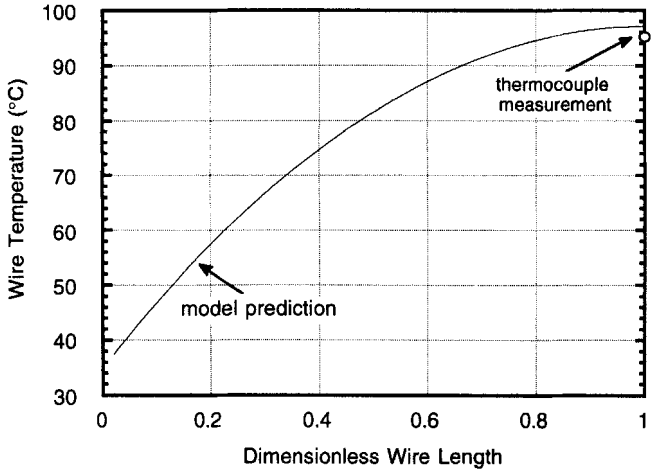

Figure 6. Wire-temperature profile for vacuum conditions.

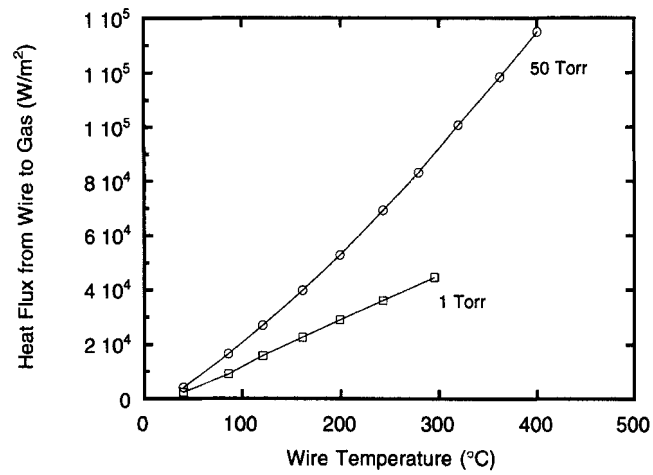

Figure 8. Heat flux from the wire center to the hydrogen gas as a function of temperature.

Table 3. Near Surface Initial Conditions after Thermal Transience

H_2 torr	WF_6 torr	SiH_4 torr	SiH_4:WF_6 Ratio	Rate torr·s^{-1}
0.375	0.147	0.106	0.72	8.15E-5
0.281	0.184	0.067	0.36	3.40E-E
*1.410	0.018	0.038	2.12	3.49E-5
0.527	0.139	0.121	0.87	1.23E-4
*0.973	0.199	0.099	0.50	6.27E-6
0.306	0.173	0.054	0.31	3.13E-5
0.88	0.198	0.99	0.50	2.94E-5
*1.344	0.024	0.044	1.83	4.85E-5
1.07	0.189	0.192	1.01	3.08E-4
0.502	0.141	0.129	0.92	1.14E-4
1.075	0.192	0.194	1.01	1.81E-4
0.417	0.139	0.122	0.88	8.80E-5
0.986	0.086	0.068	0.79	2.98E-4
0.973	0.085	0.071	0.84	2.59E-4
*0.585	0.0022	0.040	18.18	2.72E-4
0.574	0.132	0.114	0.86	2.28E-4
*0.424	0.036	0.004	0.11	3.31E-5
0.634	0.111	0.083	0.75	2.71E-4
*0.583	0.009	0.0376	4.18	1.96E-5

*Experiments not used in the regression analysis. See text for more details.

the instantaneous rate at each composition is simply the rate of decrease of the reactants, time derivative of composition, at that point. Such experiments can give hundreds of rate-composition pairs that can then be used to develop a kinetic model. The simplest rate model (not based upon a mechanism) is given as

$$\text{Rate} = k*(P_{WF_6})^n*(P_{SiH_4})^m*(P_{H_2})^p.$$

Taking the natural log of each side gives:

$$\ln(\text{rate}) = \ln k + n*\ln(P_{WF_6}) + m*\ln(P_{SiH_4}) + p*\ln(P_{H_2}).$$

For each batch experiment, the rate at early times, the initial rate, is characteristic of the rate in the absence of reaction products. As the reactants are converted and more products are generated, their influence upon the resulting rate is easily observed. In this experiment, the initial rates and their compositions were determined 130 s after the wire was heated, in order to allow thermal transience to be completed.

The initial rates and compositions, shown in Table 3, were used in a Statview multiple-regression analysis in order to determine the rate dependence on silane, tungsten hexafluoride, and hydrogen. These initial rate-regression results are shown in Table 4. The starred experiments in Table 3 were not used in the regression analysis either because the

Table 4. Statview Multiple Regression Results

	Initial Rates	All Rates
Data points used	13	1,975
r^2	0.82	0.92
SiH_4 order	1.28 ± 0.4	1.22 ± 0.01
WF_6 order	-2.40 ± 0.5	-2.17 ± 0.02
H_2 order	0.43 ± 0.3	0.27 ± 0.02

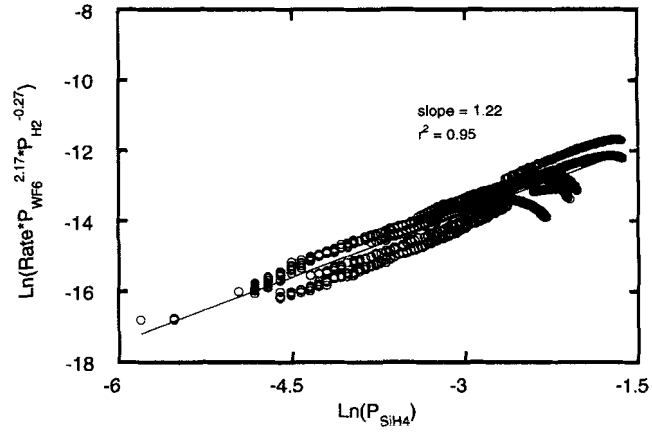

Figure 9. Dependence of the rate model on ln (silane partial pressure).
Order in silane is given by the slope.

SiH_4:WF_6 ratio was too high, indicating a reaction path other than that for depositing tungsten, or one of the species was limiting the reaction by its low concentration and mass transfer rate. A more thorough statistical analysis of the data was obtained by including every rate-composition pair throughout time for all experiments in the multiple regression. Because there was no way to calibrate the SiF_3^+ and $SiHF_2^+$ signals, the reaction products were not included in the comprehensive multiple-regression analysis. For each run, rate-composition pairs were selected from the kinetic limited regime, usually 200–300 data sets. These were all utilized in a Statview multiple-regression analysis to determine the best-fit reaction orders in silane, hydrogen, and tungsten hexafluoride. A matrix of 1,975 rates by 3 compositions was used. The resulting statistical analysis is also shown in Table 4.

The comprehensive Statview multiple regression shows that the reaction at 95°C can be modeled in a simplistic way by

$$\text{Rate(torr·s}^{-1}) = 4.15E-5*(P_{WF_6})^{-2.17}*(P_{SiH_4})^{1.22}*(P_{H_2})^{0.27}.$$

Since it is difficult to plot a multiple regression, two plots show the influence of WF_6 and silane separately. Figure 9 plots

$$\ln\left\{\text{Rate}/\left((P_{WF_6})^{-2.17}*(P_{H_2})^{0.27}\right)\right\} \text{ vs. } \ln\{P_{SiH_4}\}$$

for all pairs in all considered runs. The observed slope is the value for silane order found in the multiple regression, and the data fit the model quite well for silane pressures from 50 to 200 mtorr.

Figure 10 plots the model's relationship to WF_6 pressure:

$$\ln\left\{\text{Rate}/\left((P_{SiH_4})^{1.22}*(P_{H_2})^{0.27}\right)\right\} \text{ vs. } \ln\{P_{WF_6}\}.$$

The fit is not perfect and the displaced parallel lines probably reflect the fact that the actual initial value of WF_6 partial pressure could not be measured by the mass spectrometer.

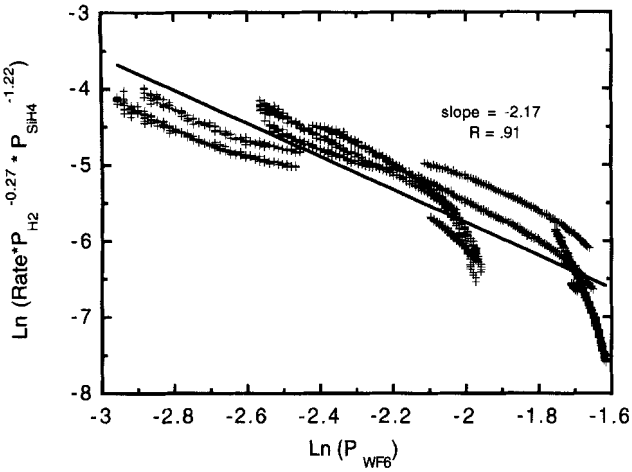

Figure 10. Dependence of the rate model on ln (WF_6 partial pressure).

Order in WF_6 is given by the slope.

While this unknown affects the intercept of each line, the slopes should be unaffected. It is clear that WF_6 inhibits the reaction rate in the range of WF_6 pressures from 50 to 200 mtorr. The variations in the data about the line suggest that this model is not complex enough to capture the true WF_6 dependence.

The rate is left in the units of torr·s^{-1}, because the true area for deposition is not known. The heated wire has a parabolic temperature profile, with different axial elements contributing their own rates. While most rates are determined by the area of maximum temperature (where the probe is placed), there are contributions from cooler elements. An accurate value for the rate coefficient can only come from masking the wire to restrict deposition to a limited and known area. The possibility that the probe measures gas dynamics corresponding to wire locations some distance away means that the measured rate may correspond to a range of temperatures.

Discussion

In each experiment, the kinetic rate dependence on concentration for a wide range of concentrations was observed as the reactants converted to products. This method for obtaining kinetic data is very efficient in terms of sample loading, gas usage, and time since over 200 instantaneous rate/composition pairs can be determined from one 30-min deposition and a few torr of gas. Because the rate is determined from gas mass balance rather than film thickness measurements, an unlimited number of rate studies can be made on one sample, saving the time and frustration of reproducing a clean substrate for every rate/composition pair, as must be done in flowing reactors. If it is necessary to confirm the gas-composition measurements of rate with film-thickness measurements, the substrate can be removed and measured. While such measurements should be made to verify the method, they defeat the efficiency gained by doing batch studies.

For most of the experiments, a single silicon fluoride product, $SiHF_3$, was produced. Significant quantities of SiF_4 appeared only when the reaction became starved for WF_6, and thus relatively rich in silane. The reactor setup readily allows identification of reaction pathways and instantaneous rates.

The power law kinetic model is only the starting point for a more complete model to be based on a surface mechanism. Because the reaction depends on all three species, it cannot be modeled by a simple adsorption limitation. The rate-limiting step is most likely a surface reaction or a desorption reaction. *In-situ* calibration of the major species will have to be done before a more detailed model can be proposed.

In all reactions, the initial rate was found to be slow and increasing until a maximum value was reached. In Figure 4, the maximum occurred at 700 s. This observation has not been made in reactors that operate at steady state. If WF_6, or one of its subfluorides, were the most abundant surface intermediate, it could significantly poison the reaction until enough was consumed for the rate-limiting step to shift. In this case, a power-law kinetic model is clearly inadequate.

In Figure 10, the rapidly increasing rate, as WF_6 is consumed at early times, is clearly seen at the high WF_6 partial pressures. For similar WF_6 partial pressures, the slope of the rate depends more on the time within a run than on the gas composition, suggesting that the mechanism is not chemical in origin. A more likely explanation is that the deposition reaction requires minimal gas-phase thermal activation, and at early times the gas is not adequately warm for the heterogeneous reaction to be rate-limiting. Rough calculations show that the species' mean free paths (≈ 0.05 mm) are on the same order as the wire diameter at 0.76 mm. In this case, Knudsen heat transfer would dominate and the gas may be very slow in reaching a steady-state temperature. It appears that gas activation may be the rate-limiting step at early times (early gas temperatures), and the surface kinetics become rate-limiting only after the gas has reached a minimal temperature.

Conclusions

A nonflowing laboratory-scale reactor has been shown to be useful in identifying reaction pathways and reaction orders during CVD. The batch mode allows observation of a wide range of instantaneous composition and chemical reaction-rate pairs with a minimal investment of time and toxic chemicals.

On the 95°C tungsten surface, tungsten was deposited and $SiHF_3$ was the primary silicon fluoride product for SiH_4 and WF_6 partial pressures from 50 to 200 mtorr, and for SiH_4/WF_6 ratios of 2 or less. Significant quantities of SiF_4 were produced when the near-surface gas composition became extremely WF_6 starved. A multiple regression fit to 1,975 composition-rate sets gave reaction orders of 1.22 in silane, 0.27 in hydrogen, and -2.17 in tungsten hexafluoride with an r^2 of 0.92. It was not possible to determine a rate constant without knowing the area of deposition as detected by the mass spectrometer. Masking the wire will resolve the problems of knowing the area and average temperature of deposition associated with this area.

The wire–gas heat-transfer characteristics reveal that the reactor operates in the Knudsen regime. Poor heat transfer, combined with the transient nature of the reactor, has revealed that the silane reduction of tungsten hexafluoride may

require minimal gas-phase thermal activation of the reactants in order for rapid deposition to occur. This is the first time such an observation has been made and could explain the differences in reported growth rates for the silane reduction reaction. No authors report the temperature history of their gases, and yet this could be critical to the reaction kinetics.

Acknowledgment

We thank the Semiconductor Research Corporation (Contract no. 90SJ178) and NSF (Contract no. GER-9023931) for their support, Dr. Derek L. Lile for the use of his mass spectrometer, and Dr. Michael J. Hafich for writing the software used to control the mass spectrometer.

Notation

P = wire perimeter, m^2
$T_{electrode}$ = temperature at ends of the wire

Literature Cited

Ammerlaan, J. A. M., P. J. Van der Put, and J. Schoonman, *Advanced Metallization for ULSI Applications 1992*, T. S. Cale and F. S. Pintchovski, eds., Mat. Res. Soc., Pittsburgh, p. 203 (1993).

Carslaw and Jaeger, *Conduction of Heat in Solids*, Clarendon Press, London (1959).

Cheek, R. W., J. G. Fleming, R. D. Lujan, R. S. Blewer, and J. A. Kelber, *Advanced Metallization for ULSI Applications 1992*, T. S. Cale and F. S. Pintchovski, eds., Mat. Res. Soc., Pittsburgh, p. 241 (1993).

Fogler, S., *Elements of Chemical Reaction Engineering*, Prentice-Hall, Englewood Hills, NJ (1992).

Kobayashi, N., H. Goto, and M. Suzuki, *J. Appl. Phys.*, **69**, 1013 (1991).

Moss, D. G., MS Thesis, Colorado State Univ., Fort Collins (1995).

Schmitz, J. E. J., M. J. Buiting, and R. C. Ellwanger, *Tungsten and Other Refractory Metals for VLSI Applications IV*, R. S. Blewer and C. M. McConica, eds., Mat. Res. Soc., Pittsburgh, p. 27 (1989).

Shon, Y., "Transient Modeling of Selective Chemical Vapor Deposition of Tungsten during a Via Filling Process," MS Thesis, Colorado State Univ., Fort Collins (1992).

Manuscript received Oct. 3, 1994, and revision received June 12, 1995.